Development 128, 3105-3115 (2001)
Printed in Great Britain © The Company of Biologists Limited 2001
DEV4550

Murine homolog of *SALL1* is essential for ureteric bud invasion in kidney development

Ryuichi Nishinakamura[1,*], Yuko Matsumoto[1], Kazuki Nakao[2], Kenji Nakamura[2], Akira Sato[1,3], Neal G. Copeland[4], Debra J. Gilbert[4], Nancy A. Jenkins[4], Sheila Scully[5], David L. Lacey[5], Motoya Katsuki[2], Makoto Asashima[3] and Takashi Yokota[1]

[1]Division of Stem Cell Regulation, Institute of Medical Science, The University of Tokyo, Tokyo 108-8639, Japan
[2]Laboratory of DNA Biology and Embryo Engineering, Institute of Medical Science, The University of Tokyo, Tokyo 108-8639, Japan
[3]Department of Life Sciences, The University of Tokyo, Tokyo 153-8902, Japan
[4]Mouse Cancer Genetics Program, National Cancer Institute at Frederick, Frederick, MD 21702-1201, USA
[5]Department of Pathology, Amgen, Thousand Oaks, CA 91320, USA
*Author for correspondence (e-mail: ryuichi@ims.u-tokyo.ac.jp)

Accepted 25 May 2001

SUMMARY

***SALL1* is a mammalian homolog of the *Drosophila* region-specific homeotic gene *spalt* (*sal*); heterozygous mutations in *SALL1* in humans lead to Townes-Brocks syndrome. We have isolated a mouse homolog of *SALL1* (*Sall1*) and found that mice deficient in *Sall1* die in the perinatal period and that kidney agenesis or severe dysgenesis are present. *Sall1* is expressed in the metanephric mesenchyme surrounding ureteric bud; homozygous deletion of *Sall1* results in an incomplete ureteric bud outgrowth, a failure of tubule formation in the mesenchyme and an apoptosis of the mesenchyme. This phenotype is likely to be primarily caused by the absence of the inductive signal from the ureter, as the *Sall1*-deficient mesenchyme is competent with respect to epithelial differentiation. *Sall1* is therefore essential for ureteric bud invasion, the initial key step for metanephros development.**

Key words: *Sall1*, Kidney, Townes-Brocks syndrome, Mouse

INTRODUCTION

Drosophila sal is the region-specific homeotic gene characterized by unique multiple double-zinc finger motifs (Kuhnlein et al., 1994). *sal* was first identified by virtue of its capacity to promote terminal differentiation (Jurgens, 1988). It is expressed in anterior and posterior compartments of *Drosophila*, and mutations in *sal* cause head and tail segments to develop trunk structures. It also plays a critical role in wing development (de Celis et al., 1996; Nellen et al., 1996). *sal* is expressed at the anterior/posterior boundary of wing imaginal discs and its expression is controlled by *dpp* (bone morphogenetic protein 4 ortholog), the expression of which is highest at the boundary, which is in turn controlled by *hedgehog* expressed in the posterior compartment. Overexpression of *dpp* broadens the expression domains of *sal*; hence, *sal* may be a downstream target of *dpp*.

Humans have at least three *sal*-related genes (*SALL1*, *SALL2* and *SALL3*) (Kohlhase et al., 1996; Kohlhase et al., 1999a). *SALL1* is located on chromosome 16q12.1 and heterozygous mutations of *SALL1* lead to Townes-Brocks syndrome, an autosomal dominant disease characterized by dysplastic ears, preaxial polydactyly, imperforate anus, and (less commonly) kidney and heart anomalies (Kohlhase et al., 1998). The incidence of kidney abnormality ranges from 20% to 62.5%, depending on the report in question (Kohlhase et al., 1999b; O'Callaghan and Young, 1995). All mutations are localized 5′ to the triple zinc-finger motif and result in premature truncation (Kohlhase et al., 1998; Kohlhase et al., 1999b; Marlin et al., 1999).

The mouse also has three Sal genes. The previously reported *msal* proved to be a homolog of human *SALL3* and was renamed *Sall3* (Ott et al., 1996; Kohlhase et al., 1999a). Homologs of *SALL1* and *SALL2* have also been reported (Buck et al., 2000; Kohlhase et al., 2000).

The kidney develops in three stages: pronephros, mesonephros and metanephros. The nephric duct (Wolffian duct) develops in a craniocaudal direction from the intermediate mesoderm and acts upon surrounding mesenchyme as an inducer of epithelial transformation to nephric tubules. The pronephric tubules, mesonephric tubules and the anterior portion of the Wolffian duct eventually degenerates; it is the metanephros that becomes the permanent kidney in mammals. Although the pronephros represents a true excretory organ in fish and amphibians, it remains a rudimentary and transient structure in the mouse. The mesonephros appears after and caudal to the pronephros. In metanephros development, the metanephric mesenchyme induces sprouting of the ureteric bud from the caudal region of the Wolffian duct. Signals from the mesenchyme cause further

branching of the ureteric bud, thus forming the kidney collecting system. Reciprocally, the ureteric bud invades the mesenchyme and induces epithelialization and differentiation of the mesenchyme into the nephron (glomerular, proximal tubular and distal tubular epithelium).

Molecular mechanisms of kidney development have been revealed mostly by gene targeting. In *Pax2* null mutants (paired-box transcription factor), the Wolffian duct develops only partially and metanephric development does not occur (Torres et al., 1995). In mice deficient for a zinc-finger transcription factor WT-1 (Wilm's tumor suppressor; Wt1 – Mouse Genome Informatics), the ureter never reaches the mesenchyme and consequently the mesenchyme undergoes apoptosis (Kreidberg et al., 1993). WT-1 is considered to control expression of signals of the mesenchyme that regulate induction and growth of the ureteric bud. A member of the TGFβ superfamily, GDNF (glial cell line-derived neurotrophic factor) expressed in the mesenchyme, acts on a receptor tyrosine kinase Ret distributed in the ureteric bud epithelium and induces branching of the ureter (Durbec et al., 1996; Trupp et al., 1996). Thus, the null mutants of GDNF and Ret show perturbation of ureter invasion (Moore et al., 1996; Pichel et al., 1996; Sanchez et al., 1996; Schuchardt et al., 1994). Reciprocal signals from the ureteric bud to the mesenchyme remained unidentified for a long period. Recently, LIF (leukemia inhibitory factor) and its related cytokines were reported to be ureter-derived regulators for mesenchymal-to-epithelial conversion, though mice deficient in the common receptor gp130 show only reduced nephron development with the initial induction occurring normally (Barasch et al., 1999). Mice that lack Wnt4 fail to form pretubular aggregates, a transitional state from mesenchyme to tubules, but other aspects of ureteric and mesenchymal development are unaffected (Stark et al., 1994). Wnt4 acts as an autoinducer of the mesenchyme-to-epithelial transition that may be activated downstream of the LIF/gp130 system. BMP7 belongs to a bone morphogenetic protein family and an initial ureter-mesenchymal interaction is unaffected in *Bmp7* mutants (Dudley et al., 1995; Luo et al., 1995). The subsequent differentiation and survival of the mesenchyme does not occur, thus indicating that BMP7 may be a maintenance signal for the mesenchyme.

Many of the genes expressed in the metanephros are also found in the pronephros. We earlier established an in vitro induction system for pronephros in *Xenopus* (Moriya et al., 1993; Uochi and Asashima, 1996). Animal caps, a presumptive ectoderm of *Xenopus* embryos at the blastula stage, differentiate into three-dimensional pronephric tubules in three days in chemically defined saline solution upon treatment with activin and retinoic acid. We have used this system to identify molecules expressed in pronephros and potentially in mesonephros and metanephros (Sato et al., 2000). One of the genes we isolated was *Xsal-3*, a newly identified *sal* member of *Xenopus*, which was expressed in the pronephros and the brain (Onuma et al., 1999). We then cloned a member of the murine Sal family from the developing kidney, which proved to be a mouse homolog of human *SALL1*. We now report cloning, expression patterns and loss-of-function studies of mouse *Sall1*. Our data show that murine *Sall1* is essential for initial inductive events for kidney development.

MATERIALS AND METHODS

Cloning of *Sall1*

Degenerate PCR was carried out using as a template 14.5 days post coitus (dpc) fetal kidney cDNA. Primers were designed for conserved regions between *Xsal-3*, *Xsal-1* and *Sall3* (EKPFACTI and WNQYAIA). The resulting 245 bp product was used to screen 14.5 dpc fetal kidney library we generated and also for the 129SvJ genomic library (Stratagene). The 5′ portion of Sall1 cDNA upstream of the first zinc finger was cloned by screening a random-primed 14.5 dpc embryo cDNA library, and the same sequence was identified in one of the genomic clones we obtained.

Interspecific mouse backcross mapping

Interspecific backcross progeny were generated by mating (C57BL/6J × *Mus spretus*) F_1 females and C57BL/6J males as described (Copeland and Jenkins, 1991). A total of 205 N_2 mice were used to map the *Sall1* locus. DNA isolation, restriction enzyme digestion, agarose gel electrophoresis, Southern blot transfer and hybridization were essentially as described (Jenkins et al., 1982). The Sall1 probe used was a *Cla*I-*Eco*RI 1.2 kb fragment (probe B). A fragment of 4.7 kb was detected in *Sph*I digested C57BL/6J DNA and a fragment of 6.1 kb was detected in *Sph*I digested *M. spretus* DNA. The presence or absence of the 6.1 kb *Sph*I *M. spretus*-specific fragment was followed in backcross mice.

A description of the probes and RFLPs for the loci linked to *Sall1*, including *Cbln1* and *Scyd1*, has been reported (Kavety et al., 1994; Rossi et al., 1998). Recombination distances were calculated using Map Manager, version 2.6.5. Gene order was determined by minimizing the number of recombination events required to explain the allele distribution patterns.

Generation of *Sall1*-deficient mice

The *Sall1*-del targeting vector was constructed by incorporating 5′ *Sma*I-*Eco*RI 5.4 kb fragment and 3′ *Hin*dIII-*Cla*I 2.8 kb fragment into a vector that contained the neomycin-resistant (neo^r) gene (pMC1-neo polyA) and a diphtheria toxin A subunit (pMC1-DTA) in tandem. The 5′ fragment was subcloned into a *Cla*I site 5′ of the neo^r gene, and the 3′ fragment was cloned into an *Eco*RV site 3′ of the neo^r gene. For the *Sall1-lacZ* construct, *Not*I-*Xho*I *lacZ* fragment (3.7 kb) from pxCAN*lacZ* (obtained from RIKEN, Japan) was fused in frame to 5′ *Sma*I-*Eco*RI 5.4 kb fragment and the resultant *Sma*I-*Xho*I 9.1 kb fragment was cloned into the *Cla*I-*Xho*I site of the vector described above. Both constructs were linearized with *Not*I.

CCE embryonic stem cells were used for the *Sall1*-del construct and E14.1 cells (provided by Dr N. Yoshida) were used for the *Sall1-lacZ* construct. CCE and E14.1 cells were plated in mitomycin C-treated STO cell lines and primary embryonic fibroblasts, respectively, and clones resistant to G418 (250 μg/ml) were screened using Southern blots. The genomic DNA from clones was digested with *Hin*dIII, electrophoresed through 0.7% agarose, transferred to nylon membrane (HybondN+, Amersham-Pharmacia), and hybridized to a radioactive probe. The probe used to screen the samples was a *Cla*I-*Eco*RI 1.2 kb fragment downstream of 3′ homology (probe B). The samples were also digested with *Bam*HI or *Xho*I, and hybridized with probe B or 5′ probe (probe A), respectively, to confirm the correct homologous recombination. A probe corresponding to the neo^r sequence was also used to verify that only one copy of the vector was integrated into the genome. Of 118 clones, eight were correctly targeted for *Sall1*-del, and 15 of 116 were targeted for *Sall1-lacZ*.

Recipient blastocysts were from C57BL/6N mice. Chimeric animals were bred with C57BL/6N females. Mutant animals studied were of F_2 and F_3 generation. Mice were genotyped using Southern blots or genomic PCR. The primer sequences used for PCR were as follows: GTACACGTTTCTCCTCAGGAC and TCTCCAGTGTGA-GTTCTCTCG for *Sall1* (200 bp); and AAGGGACTGGCTGCTAT-TGG and ATATCACGGGTAGCCAACGC for neo^r (420 bp). The

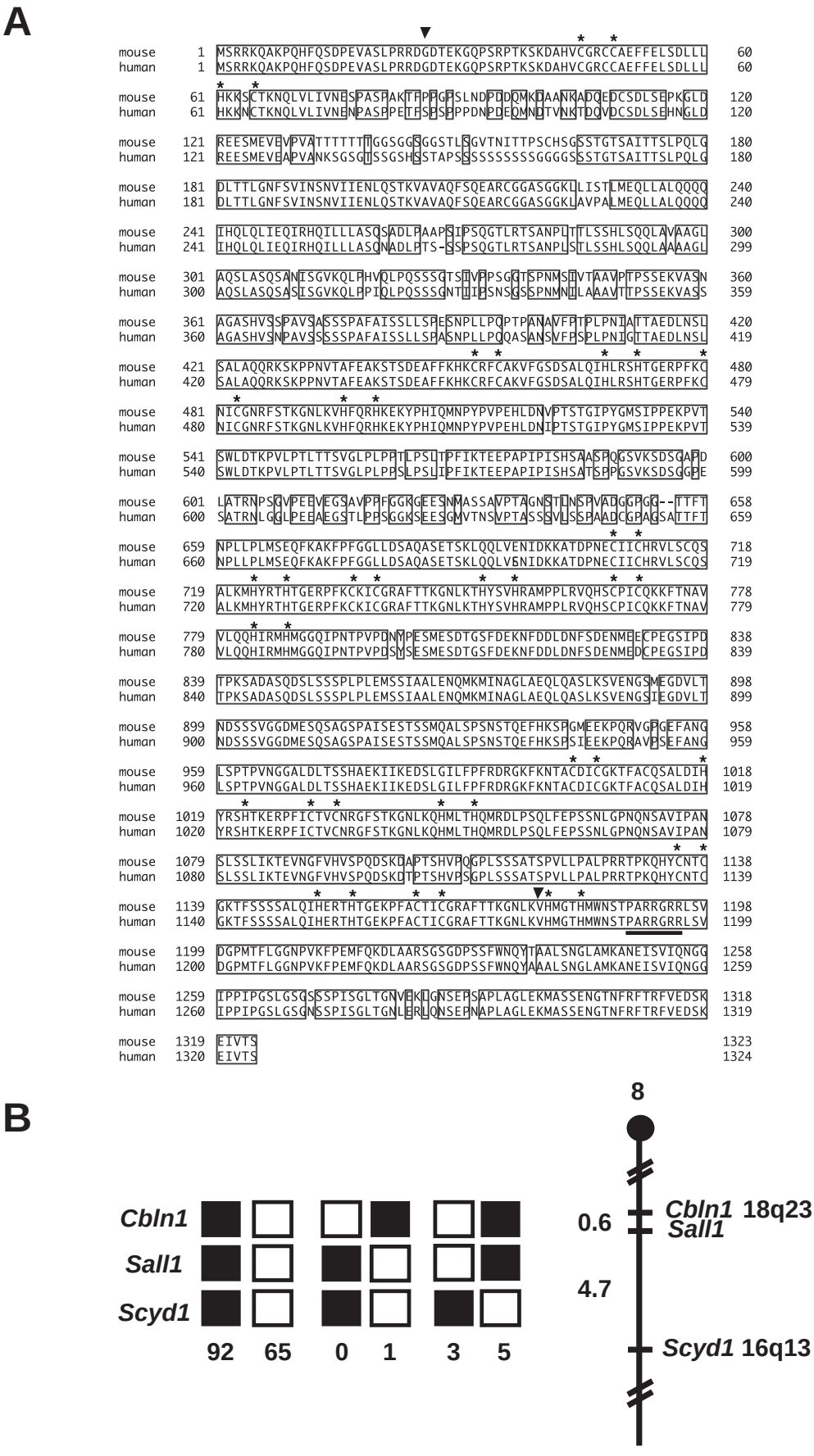

Fig. 1. Sequence and chromosomal localization of *Sall1*. (A) Amino acid sequence alignment of *Sall1* and *SALL1*. Asterisks indicate cystine and histidine residues in zinc-finger motifs. Underline indicates a putative nuclear localization signal. Black triangles are exon-intron boundaries. (B) *Sall1* maps in the central region of mouse chromosome 8. *Sall1* was placed on mouse chromosome 8 by interspecific backcross analysis. The segregation patterns of *Sall1* and flanking genes in 166 backcross animals that were typed for all loci are shown on the left of the figure. For individual pairs of loci, more than 166 animals were typed. Each column represents the chromosome identified in the backcross progeny that was inherited from the (C57BL/6J × *M. spretus*) F_1 parent. The shaded boxes represent the presence of a C57BL/6J allele and white boxes represent the presence of a *M. spretus* allele. The number of offspring inheriting each type of chromosome is listed at the bottom of each column. A partial chromosome 8 linkage map showing the location of *Sall1* in relation to linked genes is shown on the right of the figure. Recombination distances between loci in centimorgans are shown on the left of the chromosome and the positions of loci in human chromosomes, where known, are shown on the right. GenBank Accession Number for *Sall1*, AB051409.

same primers for *Sall1* were used for RT-PCR to show the absence of *Sall1* transcript.

Many *Sall1-lacZ* heterozygotes died in the perinatal period without any apparent histological abnormalities. We assume that death was probably due to the toxicity of *lacZ*, as such lethality was not observed in *Sall1*-del heterozygotes. The surviving *Sall1-lacZ* heterozygotes bred normally and resultant homozygous mice showed phenotypes identical to those of *Sall1*-del homozygous mice.

Histological examination

Samples were fixed in 10% formalin and processed for paraffin-embedded sectioning (6 μm), followed by double staining with Hematoxylin and Eosin. X-gal staining was as described (Koseki et al., 1991). All of the X-gal staining patterns

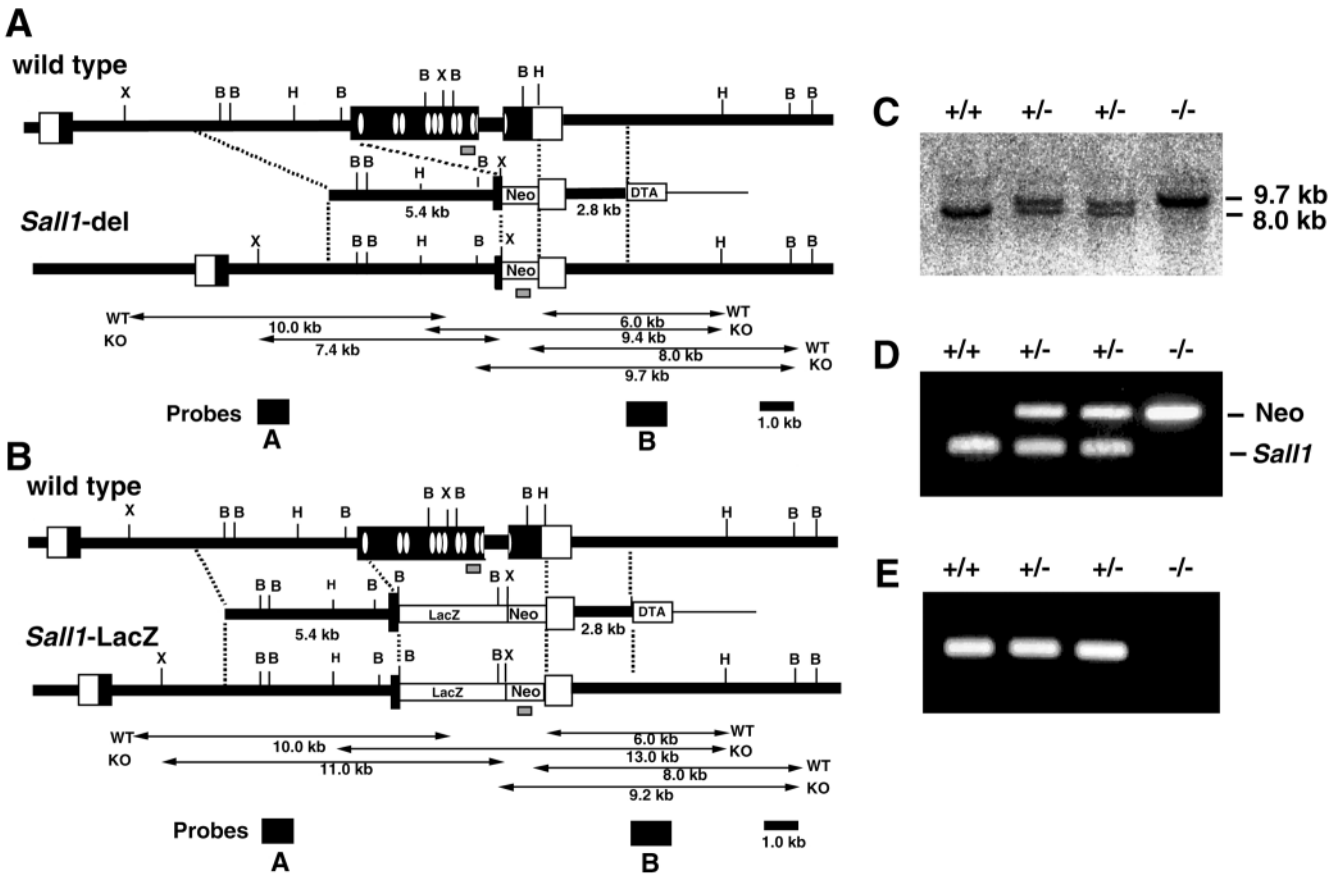

Fig. 2. Generation of *Sall1*-deficient mice. (A) Targeting strategy of *Sall1*-del. Positions of zinc finger motifs are indicated as ovals. (B) Targeting strategy of *Sall1-lacZ*. (C) Southern blot analysis of wild-type (+/+), heterozygous (+/–), homozygous (–/–) *Sall1*-del mutant mice. Tail DNA was digested with *Bam*HI and hybridized with probe B. (D) Genomic PCR of wild-type (+/+), heterozygous (+/–), homozygous (–/–) *Sall1*-del mutant mice. The 420 bp band was amplified from neo^r gene and the 200 bp band was from *Sall1* genome. The positions of the PCR products are indicated as gray bars. (E) RT-PCR of *Sall1* transcript in wild-type (+/+), heterozygous (+/–), homozygous (–/–) *Sall1*-del mutant mice.

of heterozygous *Sall1-lacZ* mice described were reconfirmed by in situ hybridization. For detection of apoptosis, ApopTag Fluorescein Direct Kits (Intergen) were used for paraffin-embedded sections and counterstained with Propidium Iodide. Omission of terminal deoxynucleotidyl transferase gave no background signals.

In situ hybridization

In situ hybridization was carried out using digoxigenin-labeled antisense riboprobes. Samples were fixed overnight in 4% paraformaldehyde (PFA) in phosphate-buffered saline (PBS), then in sucrose and embedded with OCT compound. Sections were cut, air-dried and then fixed in 4% PFA for 15 minutes at room temperature. After washing with PBS, sections were treated with proteinase K (5 μg/ml for 15 minutes), refixed with PFA, washed with PBS, treated with 0.2 M hydrochloride for 10 minutes and washed again with PBS. Samples were acetylated for 10 minutes, washed with PBS and dehydrated with ethanol. Hybridization mixture (50% formamide, 10 mM Tris-HCl pH 7.6, 200 μg/ml tRNA, 1× Denhardt's solution, 10% dextran sulfate, 600 mM NaCl, 0.25% SDS, 1 mM EDTA, and the probe) was then applied on top of the section, overlaid with parafilm, and incubated overnight at 70°C in a humidified chamber. Sections were washed for 30 minutes with 2×SSC/50% formamide at 70°C, treated with RNase for 30 minutes at 37°C, washed with 2×SSC for 20 minutes at 70°C and washed twice with 0.2×SSC for 20 minutes each at 70°C. Sections were rinsed with buffer 1 (100 mM Tris-HCl pH7.5, 150 mM NaCl), blocked with 10% sheep serum in buffer 1 for 1 hour and incubated with alkaline phosphatase-conjugated sheep polyclonal antidigoxigenin antibody (Roche) diluted 1:4000 in buffer 1 for 30 minutes. After washing twice with buffer 1, alkaline phosphatase activity was detected in the presence of NBT/BCIP (Roche).

A 800 bp *Xho*I-*Spe*I fragment of Sall1 cDNA was subcloned into pBluescript II KS- (Stratagene) and a transcript was generated with T7 polymerase. Wnt4 was a gift from Dr Andrew P. McMahon. cDNA for other probes was isolated by PCR, subcloned into pCRII (Invitrogen) and sequenced. None of the sense probes produced any signals.

Organ culture of metanephric mesenchyme

Metanephric rudiments are dissected from 11.5 dpc embryos and cultured at air-fluid interface on Transwell (0.4 μm) (Corning) supplied with DMEM plus 10% fetal calf serum. For recombination experiments with spinal cord, mesenchyme at 11.25 dpc was used to minimize apoptosis in the mutants. The mesenchyme was removed from the ureteric bud after 5 minutes incubation with 0.2% collagenase (Sigma) and cultured in direct contact with spinal cord on Transwell. As a specific size of the mesenchyme is required for the efficient response to spinal cord, left and right mesenchyme were combined and cultured.

GenBank Accession Number

The DDBJ/EMBL/GenBank Accession number for the *Sall1* cDNA sequence reported in this paper is AB051409.

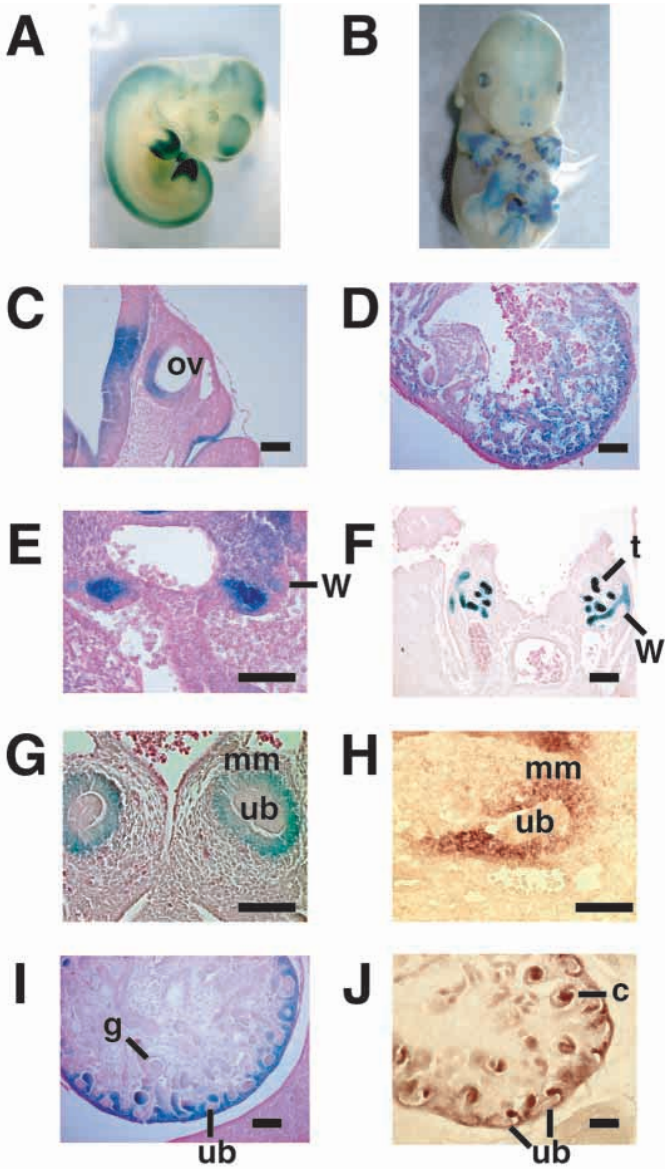

Fig. 3. Expression of *Sall1* in developing embryos. (A-G,I) X-gal staining and (H,J) in situ hybridization of *Sall1-lacZ* heterozygous mice. (A) Lateral view of embryo at 11.5 dpc. (B) Ventral view of embryos at 14.5 dpc. (C) Otic vesicle at 10.5 dpc (ov, otic vesicle). (D) Heart at 11.5 dpc. (E) Nephrogenic primordium at 10.5 dpc (W, Wolffian duct). (F) Mesonephros at 11.5 dpc (t, mesonephric tubule). (G) Metanephros at 11.5 dpc (mm, metanephric mesenchyme; ub, ureteric bud). (H) Metanephros at 11.5 dpc (in situ hybridization). (I) Metanephros at 14.5 dpc (g, glomerulus). (J) Metanephros at 14.5 dpc (in situ hybridization) (c, comma-shaped bodies). Scale bars: 100 μm.

RESULTS

Cloning of a mouse homolog of *SALL1* (*Sall1*)

We isolated a murine *sal* cDNA encoding 1323 amino acids from a fetal kidney cDNA library (Fig. 1A). There were four characteristic double zinc-finger motifs, the second of which had triple zinc fingers, and it also had a single zinc-finger motif at its N terminus. It had a putative nuclear localization signal in the C-terminal region, and GFP fusion protein was localized exclusively in the nucleus when expressed in COS cells (Fig. 1A and data not shown). This gene was 90% identical at the amino acid level to human *SALL1*, a causative gene for Townes-Brocks syndrome. Interspecific backcross analysis showed that this mouse gene was localized in the central region of mouse chromosome 8 linked to *Cbln1* and *Scyd1* (Fig. 1B). This region is homologous to human chromosome 18q and 16q, the latter of which is the location of *SALL1*, further supporting the assumption that it is a murine homolog of *SALL1*. Fluorescent in situ hybridization analysis also confirmed that it was localized on mouse chromosome 8 (data not shown). Recently, Buck et al. have reported a murine homolog of *SALL1*; their clone is practically identical to ours, albeit with minor nucleotide differences (Buck et al., 2000).

Generation of *Sall1*-deficient mice

To examine developmental functions of this mouse homolog of *SALL1*, we inactivated it in the mouse using embryonic stem cells (Fig. 2A, B). *Sall1* gene consists of three exons, the first intron being approximately 9 kb. Most zinc-finger domains are located in exon 2 and the last 10th zinc-finger domain is separated by a short second intron. We generated two types of targeting constructs: one deleted the entire coding sequence, except for the N-terminal 52 amino acids, thus eliminating all the zinc-finger motifs (*Sall1*-del); the other deleted the same region and *lacZ* was fused in frame to N-terminal 52 amino acids (*Sall1-lacZ*). Homologous recombinants were obtained from both constructs and chimeras from both transmitted the mutations through the germline. Mutant mice from the two constructs showed essentially the same phenotypes. Mice were genotyped by Southern blots and genomic PCR (Fig. 2C, D). RT-PCR revealed the absence of the *Sall1* transcript in the homozygous mutant mice (Fig. 2E). In situ hybridization also confirmed the absence of the *Sall1* transcript, but not *Sall2*, in the mutant mice (data not shown).

Expression patterns of *Sall1*

Whole-mount X-gal staining of *Sall1-lacZ* heterozygous embryo at 11.5 dpc showed abundant expression of *Sall1* in limb buds and a relatively weaker signal in the spinal cord and the brain (Fig. 3A). Staining of 14.5 dpc embryo showed expression in limb buds, anorectal region, developing olfactory bulb, nose and eye (Fig. 3B). Transverse section of 10.5 and 11.5 dpc showed *Sall1* staining in ventromedial parts of otic vesicles and endocardium (Fig. 3C,D). In kidney development, *Sall1* expression was observed in the nephrogenic primordium at 10.5 dpc (Fig. 3E). At 11.5 dpc, *Sall1* was expressed in mesonephric tubules and Wolffian ducts, and in the metanephric mesenchyme surrounding the ureteric bud (Fig. 3F,G), findings that were reconfirmed by in situ hybridization (Fig. 3H). Expression of *Sall1* was reduced in the caudal area of the Wolffian duct and was undetectable in ureteric buds. At 14.5 dpc, *Sall1* expression was observed in the mesenchyme around the ureteric buds and weakly in comma-shaped bodies of metanephric tubules, but not in glomeruli, in the cortical regions of the developing kidney (Fig. 3I,J). In the newborn, *Sall1* staining was observed in kidneys, hearts, livers, brain regions surrounding ventricles and olfactory bulbs (data not shown). All this evidence was reconfirmed by in situ hybridization. Thus, *Sall1-lacZ* mice serve as useful tools to

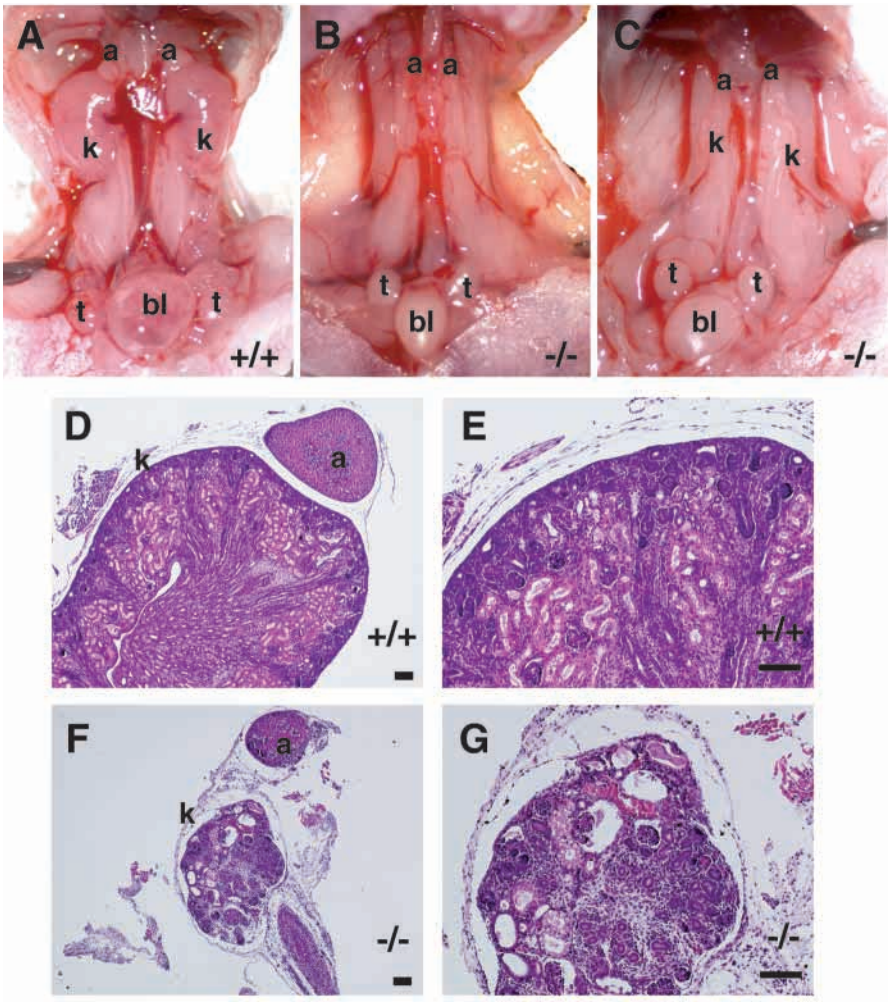

Fig. 4. Kidney phenotypes in *Sall1*-deficient mice. (A) Kidneys of wild-type newborn. Urinary bladder is filled with urine. (B) Kidneys of *Sall1*-deficient newborn. Note kidneys are completely absent and the urinary bladder is not inflated with urine. Other organs, such as adrenal glands and testis, are normal. (C) Kidneys of another *Sall1*-deficient newborn with severe bilateral kidney hypoplasia. Urine is absent from the bladder. (D,E) Histological examination of kidney in wild-type mice. (F,G) Histological examination of hypoplastic kidney in *Sall1*-deficient mice. a, adrenal gland; bl, urinary bladder; k, kidney; t, testis. Scale bars: 100 μm

monitor *Sall1* expression and *Sall1* was shown to be expressed in tissues affected in Townes-Brocks syndrome, namely limb, ear, anus, heart and kidney. This expression pattern partly overlaps that of mouse *Sall2* (data not shown) and *msal* (*Sall3*) (Ott et al., 1996; Ott et al., 2001).

Kidney defects in *Sall1*-deficient mice

Homozygous mice were born at Mendelian frequency but all died within 24 hours after birth without suckling. Kidney agenesis or severe dysgenesis were present (Fig. 4). Nine out of 28 mice (32.1%) had no kidneys or ureters, bilaterally (Fig. 4B). Eight mice (28.6%) had unilateral kidney agenesis and hypoplasia on the other side. Eleven mice (39.3%) had two small remnant kidneys (Fig. 4C). In either case, the bladder contained no urine. Histological examination of the remnant kidneys showed a disorganized cortical structure, shrunken glomeruli, necrotic proximal tubules and multiple cysts (Fig. 4F,G). Development of other organs including brain, adrenal glands, bladder, testis or ovary was normal. There was no limb deformity, anorectal anomaly or ear anomaly, all characteristic of Townes-Brocks syndrome. The layer structure of olfactory bulbs in *Sall1* mutant newborn mice was slightly disorganized, though adult phenotypes of *Sall1* mutation could not be determined, owing to the lethality of the mutant mice (data not shown).

At day 11.5 of gestation, the ureteric bud invades into metanephric mesenchyme and subsequent reciprocal interaction between these two tissues leads to development of a metanephric kidney (Fig. 5A). In the *Sall1*-null mice, mesonephros development was normal and morphologically distinct metanephric mesenchyme was formed, albeit reduced in size (Fig. 5B). By contrast, the ureteric bud formed but failed to invade the metanephric mesenchyme. Subsequent differentiation of mesenchyme and branching of the ureteric bud did not occur on either side (44.4%, n=18). Some mutants showed invasion of ureteric bud on one side (38.9%) or both (16.7%), but mesenchymal condensation and ureteric branching were significantly poorer than in wild-type littermates (Fig. 5C). Consequently, at day 12.5 and 14.5 of gestation, kidneys in mutant mice were absent or small, with poorly differentiated tubules and ureteric components (Fig. 5D-I). Furthermore, several apoptotic cells with dark nuclear fragments were found in the mesenchyme at 11.5 dpc and TUNEL analysis confirmed apoptosis in the mesenchyme at this stage (Fig. 5J,K). Thus, loss of *Sall1* leads to a failure of ureteric bud invasion into mesenchyme and subsequent apoptosis of the mesenchyme. This phenotype is more severe than findings in mutant mice deficient in Wnt4, or BMP7, in which ureter-mesenchyme interaction does occur to some extent. The variability of the phenotypes may be due to the mixed genetic background of the animals analyzed or to residual activity of other Sall genes. *Sall2* and *Sall3* were expressed in developing kidney (data not shown).

Heterozygous mice were apparently normal and did not show phenotypes of Townes-Brocks syndrome, such as dysplastic ears, preaxial polydactyly, imperforate anus and renal anomaly.

Downregulation of metanephric mesenchymal genes in *Sall1*-deficient mice

To examine kidney phenotypes in more detail, we next examined expression patterns of several well-characterized

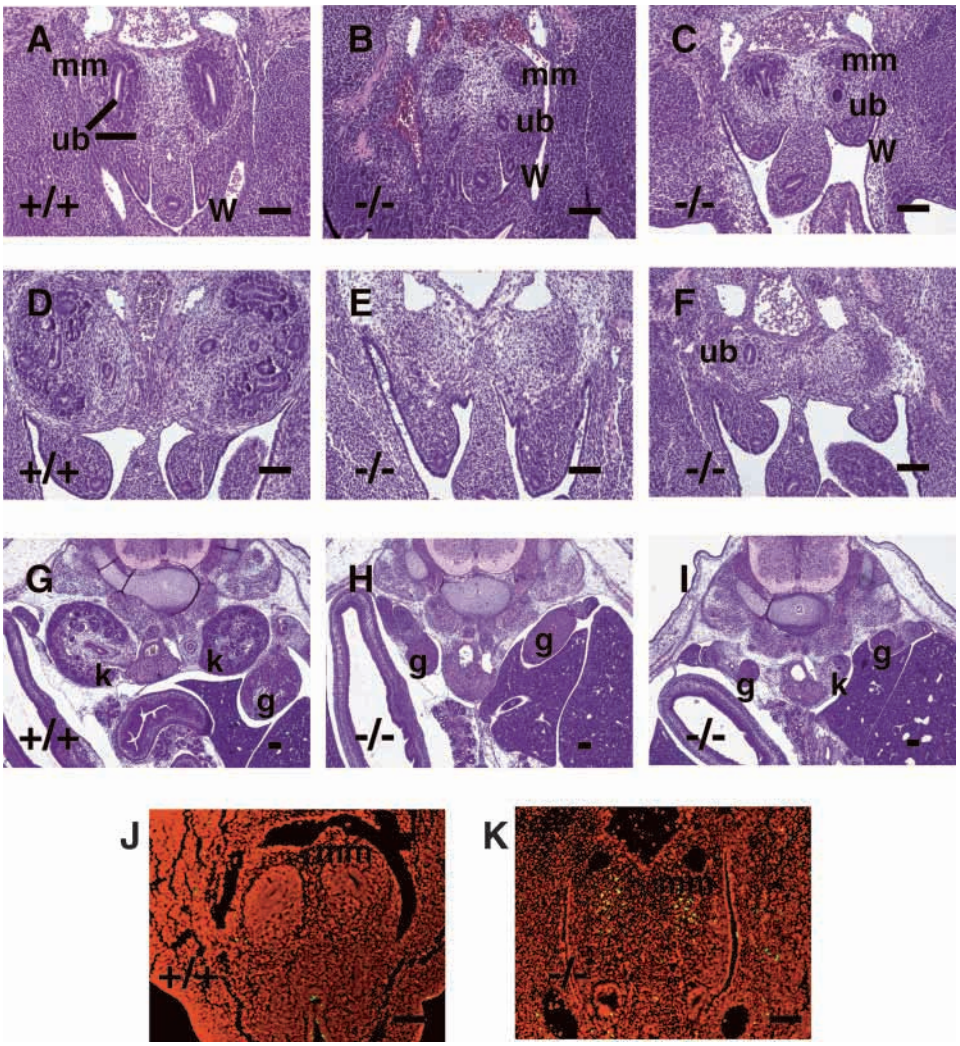

Fig. 5. Kidney development in *Sall1*-deficient mice. (A) Metanephros in wild-type mice at 11.5 dpc. Ureteric bud (ub) branches from Wolffian duct (W) and metanephric mesenchyme (mm) are condensed around the bulging ureteric bud. (B) Metanephros in *Sall1*-deficient mice at 11.5 dpc. Metanephric mesenchyme is formed but reduced in size and is not invaded by the ureteric bud. (C) Metanephros in *Sall1*-deficient mice at 11.5 dpc. The left ureteric bud invades the mesenchyme, but does not bulge. (D) Metanephros in wild-type mice at 12.5 dpc. Branching of ureter is evident. (E) Metanephros in *Sall1*-deficient mice at 12.5 dpc. No kidney is detected. (F) Metanephros in *Sall1*-deficient mice at 12.5 dpc. Ureteric bud is observed in the left primordium, but no branching occurs. (G) Metanephros in *Sall1*-deficient mice at 14.5 dpc (k). Cortex and medullar regions are formed and glomeruli are observed. (H) Metanephros in *Sall1*-deficient mice at 14.5 dpc. Kidney is absent though gonads (g) are present. (I) Metanephros in *Sall1*-deficient mice at 14.5 dpc. A small kidney with poorly branched tubules and ducts is observed on the right. (J) TUNEL analysis of metanephros in wild-type mice at 11.5 dpc. TUNEL analysis of metanephros in *Sall1*-deficient mice at 11.5 dpc. Note the yellow apoptotic cells in the mesenchyme. Scale bars: 100 μm

molecular markers of either mesenchyme or ureteric bud-derived cells.

Pax2-deficient mice do not develop mesonephric tubules and lack ureteric buds (Torres et al., 1995). In metanephros at 11.5 dpc, *Pax2* is expressed both in ureteric bud and condensed mesenchyme surrounding the ureteric bud (Fig. 6A). In *Sall1* mutant mice, expression of *Pax2* was unaltered in the ureteric bud, though no bulging of ureteric bud tip was observed (Fig. 6B). Expression domain size of the mesenchymal component of *Pax2* was significantly reduced, thereby reflecting the size of the mesenchyme. Thus, *Pax2* expression in the mutant mice was consistent with the histological characteristics: failure of the ureteric bud to invade and reduced size of the mesenchyme.

Mice deficient in the tyrosine-kinase type receptor, Ret, as well as its ligand GDNF, show failure of ureteric bud invasion and subsequent failure of mesenchymal differentiation (Moore et al., 1996; Pichel et al., 1996; Sanchez et al., 1996; Schuchardt et al., 1994). Ret was exclusively expressed in the ureteric bud in the wild type, and its expression in *Sall1* mutant mice was unaltered, though bulging of ureteric bud tip was not evident (Fig. 6C,D). This result, together with that of ureteric bud component of Pax2, indicates that markers of ureteric bud were not affected in the absence of *Sall1*.

GDNF is a ligand for Ret and is expressed in the metanephric mesenchyme. GDNF is weakly expressed in the uninduced mesenchyme and strongly upregulated upon ureteric bud invasion (Fig. 6E). *Sall1* mutant mice showed a reduced expression of GDNF at 11.5 dpc (Fig. 6F). GDNF expression before ureteric bud invasion (10.5 dpc) was, however, unaffected in the mutant mice (data not shown). Expression of Eya1, a putative upstream molecule of GDNF (Xu et al., 1999), was not significantly affected in the mutants at 10.5 or 11.5 dpc, except for the reduced size of the expression domain at 11.5 dpc (data not shown).

BMP7-deficient mice show normal initial metanephric induction, though the size of the kidney is reduced (Dudley et al., 1995; Luo et al., 1995). BMP7 is expressed both in the ureteric bud and in the mesenchyme (Fig. 6G). In *Sall1* mutant mice, BMP7 expression was reduced in the mesenchyme and relatively unaffected in the ureteric bud (Fig. 6H).

Wnt4 is required for epithelialization of the induced mesenchyme but not for the initial induction by ureter (Stark et al., 1994). It is expressed in mesenchymal cells on sides of the ureteric bud at 11.5 dpc and correlates to the site where the first pretubular aggregates form (Fig. 6I). *Sall1*-deficient mice showed significantly reduced Wnt4 expression (Fig. 6J).

WT-1 is expressed in the metanephric mesenchyme and its

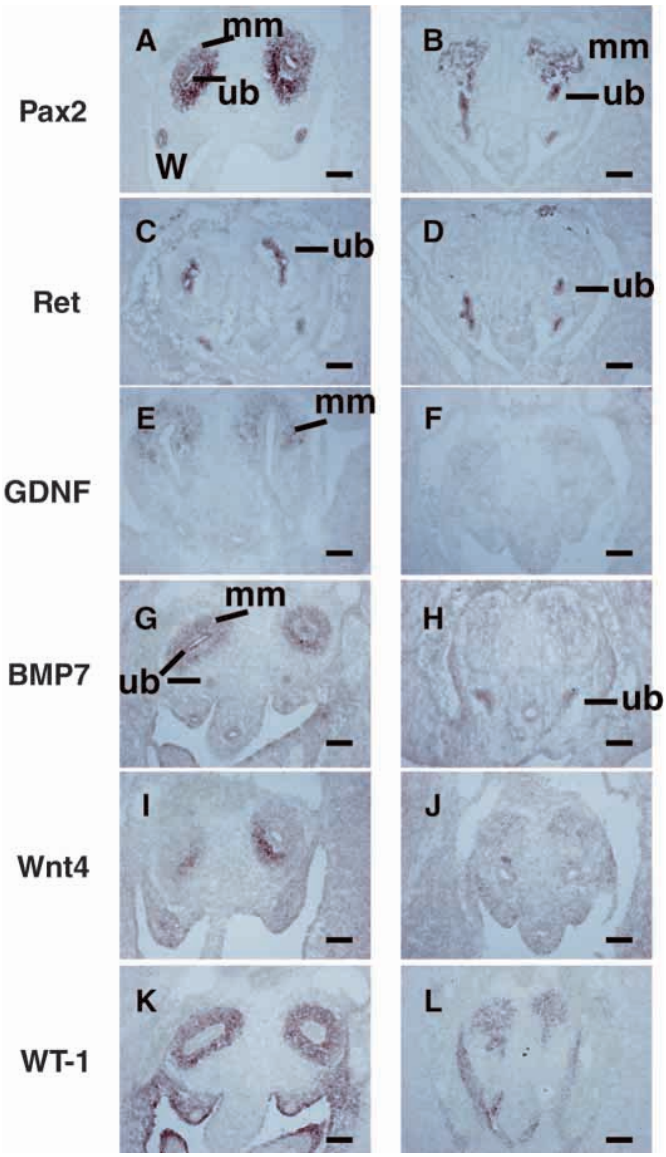

Fig. 6. In situ hybridization of molecular markers in 11.5 dpc metanephros of wild-type (left columns, A,C,E,G,I,K) and *Sall1*-deficient mice (right columns, B,D,F,H,J,L). (A,B) Pax2, (C,D) Ret, (E,F) GDNF, (G.H) BMP7, (I.J) Wnt4 and (K,L) WT-1. Scale bars: 100 μm.

absence leads to failure of mesenchymal induction (Kreidberg et al., 1993). Expression domain size of WT-1 was also significantly reduced in the absence of *Sall1* (Fig. 6K,L).

Thus, *Sall1* deficiency led to remarkable downregulation of some mesenchymal markers (GDNF, BMP7, Wnt4) and reduced size of expression domain of others (Pax2 and WT-1). These data are consistent with histological findings that *Sall1* mutant metanephric mesenchyme was significantly reduced in size and was not invaded by the ureteric bud. Downregulation of the markers suggests that the mutant mesenchyme is not induced properly by signals from the ureteric bud. None of the mesenchymal markers was, however, completely absent, but was reduced, thus indicating that specification of the mesenchyme occurs in *Sall1* deficiency.

Tubule induction in *Sall1*-deficient metanephric mesenchyme

To further demonstrate that kidney development is impaired in *Sall1* deficient mice at the initial stage, kidney rudiments were isolated from *Sall1* mutant mice at 11.5 dpc and cultured in vitro (Fig. 7A-C). All wild-type or heterozygous rudiments developed into a fully branched kidney structure in 3 days (n=7 and n=20, respectively). *Sall1* mutants, however, formed no (n=9) or only small numbers (n=5) of branched structures (if any), findings that are consistent with phenotypes in vivo.

To determine if the kidney abnormality in *Sall1*-deficient mice was due to an autonomous cell defect of metanephric mesenchyme, or to the imcomplete invasion of the ureteric bud that is a normal inducer, the mutant mesenchyme was recombined with the spinal cord. The mesenchyme cultured in vitro degenerates when removed from the ureteric bud. When recombined with the spinal cord, however, 11 out of 11 wild-type and 15 of 16 heterozygous mesenchymes formed renal tubules within 5 days, as shown in Fig. 7D (Saxen, 1987). Wnt family members expressed in spinal cord bypass the inductive signal from the ureter by mimicking the normal mesenchymal action of Wnt4 (Kispert et al., 1998). Eleven out of 12 metanephric mesenchymes from *Sall1*-deficient mice formed renal tubules when recombined with the wild-type or heterozygous spinal cord – independent of the severity of the ureteric invasion impairment (Fig. 7E). This indicates that the *Sall1*-deficient mesenchyme is competent with respect to epithelial transformation. Induced mutant tubules were consistently smaller than those of wild type or heterozygotes, perhaps because of reduced cell number of the mutant mesenchyme at the time of dissection. These data demonstrate that there is no inherent defect in the ability of *Sall1*-deficient metanephric mesenchyme to make tubules upon induction; thus, the kidney phenotype of the *Sall1*-deficient mice is likely to be primarily caused by the lack of invasion of the ureteric bud that is a normal inducer.

DISCUSSION

Our data indicate that *Sall1* is required for initial interaction between the ureter and the metanephric mesenchyme, though phenotypes of the mutants were variable, as in cases of some knockouts with kidney phenotypes. For example, only one-third of the newborn Ret mutants show complete absence of ureter and kidney, and one-tenth have bilateral kidney rudiments (Schuchardt et al., 1994). Ret mutants also show a range of defects in formation, growth and branching of the ureteric bud at the initial stage of metanephros formation (Schuchardt et al., 1996). Some of the GDNF mutants do develop ureteric buds that invade the mesenchyme (Moore et al., 1996; Pichel et al., 1996; Sanchez et al., 1996). The phenotype variability may be due to redundant functions of related molecules or to a mixed genetic background of the animals examined.

Based on impaired invasion of the ureteric bud in *Sall1*-deficient kidney (Fig. 5) and responsiveness of *Sall1*-null mesenchyme to spinal cord-derived signal in organ culture (Fig. 7), loss of *Sall1* expression in the mesenchyme is likely to lead to failure to attract the ureteric bud that is a normal inducer, and to subsequent failure of tubule differentiation in

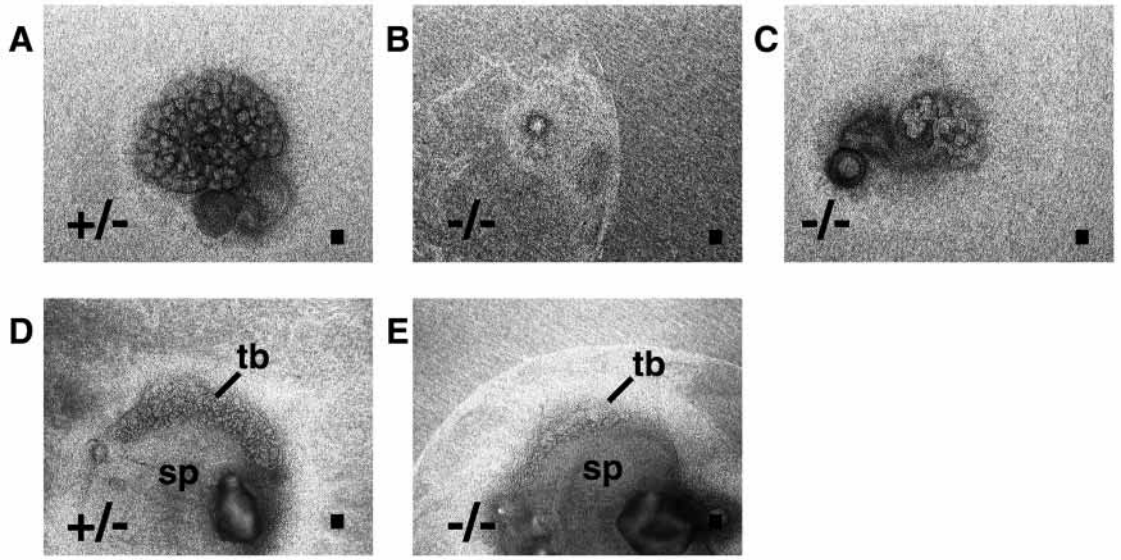

Fig. 7. Organ culture of *Sall1*-deficient metanephric mesenchyme. (A) Heterozygous metanephric rudiment cultured for 3 days. (B) *Sall1*-deficient metanephric rudiment cultured for 3 days. Only residual ureter is evident. (C) *Sall1*-deficient metanephric rudiment cultured for 3 days. A limited branching is observed. (D) Heterozygous metanephric mesenchyme cultured with spinal cord for 5 days. (E) *Sall1*-deficient metanephric mesenchyme cultured with heterozygous spinal cord for 5 days. sp, spinal cord; tb, renal tubules. Scale bars: 100 μm.

the mesenchyme. Reduced but persistent expression of early mesenchymal markers is also consistent with this model.

The most severe cases of *Sall1* knockout were similar to those of GDNF or WT-1 deficient mice. GDNF is expressed in the metanephric mesenchyme and is a key molecule for attracting ureteric bud, which acts through the Ret receptor. Thus, GDNF knockouts show failure of ureteric bud invasion. GDNF expression in the mesenchyme is reduced in *Sall1* knockout at 11.5 dpc, but not at 10.5 dpc (before ureteric bud invasion). This indicates that *Sall1* is not absolutely required for GDNF expression. Furthermore, expression of Eya1, an upstream molecule of GDNF, is relatively unaffected in the mutants. Therefore, GDNF reduction in *Sall1* mutants, which could lead to incomplete ureteric bud invasion, is not likely to be caused by a direct effect of *Sall1* on GDNF expression.

WT-1 is also expressed in the metanephric mesenchyme, and its absence leads to failure of ureteric bud invasion and apoptosis of the mesenchyme. WT-1 expression in *Sall1*-deficient mice was, however, weakly detected, though reduced, thus indicating that *Sall1* is not essential for WT-1 expression. Furthermore WT-1 knockout show extrarenal phenotypes such as abnormal heart, lung and gonad development, which were not observed in the *Sall1* knockouts. Therefore, *Sall1* is unlikely to be upstream of WT-1. It is still possible that *Sall1* is a downstream effector of WT-1, or that *Sall1* and WT-1 are synergistic for metanephric development.

Identification of downstream direct targets of *Sall1* is needed to fully explain kidney phenotypes of *Sall1*-deficient mice. *Sall1* contains 10 zinc-finger motifs, most of which are clustered in duplex or triplet. It is not known which zinc-finger domain is involved in DNA binding or in transactivation. Some sets of zinc fingers may bind to DNA and other sets may serve for protein-protein interactions, as in the case of Olf-1 associated zinc finger (OAZ), which has 30 zinc fingers (Hata et al., 2000). OAZ uses different zinc fingers depending on target promoters and *Sall1* may use similar mechanisms. *Drosophila spalt-related* (*salr*) binds to an A/T-rich consensus sequence through its triplet zinc fingers, but endogenous targets have not been identified (Barrio et al., 1996). *Drosophila sal/salr* is reported to regulate the expression of *knirps* and *iroquios* in wing veins, but direct binding of *sal/salr* to their promoters was not seen (Lunde et al., 1998; de Celis and Barrio, 2000). A search for *Sall1* target genes is under way in our laboratory.

In *Drosophila* wing imaginal discs, *sal* is located downstream of *dpp*, which is a BMP4 ortholog (de Celis et al., 1996; Nellen et al., 1996). BMP7 is the major BMP family gene expressed in mouse developing kidney and is essential for kidney development (Dudley et al., 1995; Luo et al., 1995). It is tempting to speculate that *Sall1* expression is controlled by BMP7. The kidney phenotype of *Sall1* knockout is, however, more severe than that of BMP7 knockout. In addition BMP7 deficient mice show eye abnormality, which is not observed in *Sall1*-deficient mice. Therefore, *Sall1* is unlikely to be a downstream signaling component of BMP7.

Recently, *sal* was found to be downstream of the *wingless* signal in the *Drosophila* tracheal system and *sal* deletion results in absence of dorsal trunks of the trachea (Chihara and Hayashi, 2000; Llimargas, 2000). Though Wnt4 is essential for kidney development, a normal ureter-mesenchyme interaction occurs in its mutants, which is different from phenotypes of *Sall1*-deficient mice (Stark et al., 1994). Furthermore *Sall1* is not expressed in trachea and lungs, and *Sall1*-deficient mice apparently have no lung defects. Therefore, the simple analogy of *Drosophila* does not apply to mammals.

LIF and related cytokines are ureter-derived regulators for mesenchymal-to-epithelial conversion (Barasch et al., 1999). *Sall1* expression was, however, unaffected in mice deficient in gp130, the common receptor for LIF family cytokines (data not shown). Furthermore the kidney phenotype of gp130-deficient mice is much milder than that of *Sall1*-deficient mice (Barasch

et al., 1999). Thus, *Sall1* is unlikely to be downstream of the LIF/gp130 signal. Identification of molecules that govern the expression of *Sall1* in mesenchymal cells will be important for understanding mechanisms of kidney development: *Sall1-lacZ* heterozygous mice represent be powerful tools with which to achieve this.

We have found almost no abnormality in *Sall1* mutant mice except for that in the kidney, despite abundant expression in various tissues. Expression of GDNF, BMP7, Pax2, Wnt4 in other regions, such as in the brain and spinal cord, remained intact in the *Sall1* mutant mice (data not shown). As some of expression patterns of *Sall2* and *Sall3* overlapped those of *Sall1*, they may compensate for each other. Elimination of these other Sall gene family members would elucidate their roles in other tissues as well as in the kidney.

Another intriguing point is that heterozygous mutant mice do not show similar phenotypes of Townes-Brocks syndrome therefore cannot serve as a disease model for human disease. Even phenotypes of homozygous mutant mice differed from those of the human disease. The relative importance of *SALL1* over *SALL2* and *SALL3* may be higher in humans than in mice, and *Sall1* deficiency may be compensated for by *Sall2* and *Sall3* in mice. Alternatively, heterozygous mutations in humans, which result in premature truncation 5′ to the triple zinc-finger motif, may serve in a dominant-negative fashion and eliminate functions of all SALL genes. To test these hypotheses, generating transgenic mice carrying a truncated *Sall1*, as well as deleting all Sall genes in mice, would be necessary. Nonetheless, the kidney phenotypes observed in Townes-Brocks syndrome are likely to be explained by the essential role of *SALL1* in the initial key step of kidney development. Elucidation of upstream and downstream molecular events will lead to better understanding of kidney development, as well as to finding potential therapy targets for individuals with this disease.

We thank Dr T. Hara for critical reading of the manuscript, Drs M. Nakafuku and T. Ishihara for advice, Y. Chida, M. Emoto and D. B. Householder for technical support, and M. Ohara for language assistance. The Division of Stem Cell Regulation is supported by Amgen Limited.

REFERENCES

Barasch, J., Yang, J., Ware, C. B., Taga, T., Yoshida, K., Erdjument-Bromage, H., Tempst, P., Parravicini, E., Malach, S., Aranoff, T. and Oliver, J. A. (1999). Mesenchymal to epithelial conversion in rat metanephros is induced by LIF. *Cell* **99**, 377-386.

Barrio, R., Shea, M. J., Caruli, J., Lipkow, K., Gaul, U., Frommer, G., Schuh, R., Jackle, H. and Kafatos, F. C. (1996). The *spalt*-related gene *of Drosophila melanogaster* is a member of an ancient gene family, defined by the adjacent, region-specific homeotic gene *spalt*. *Dev. Genes Evol.* **206**, 315-325.

Buck, A., Archangelo, L., Dixkens, C. and Kohlhase, J. (2000). Molecular cloning, chromosomal localization, and expression of the murine *SALL1* ortholog *Sall1*. *Cytogenet. Cell Genet.* **89**, 150-153.

Chihara, T. and Hayashi, S. (2000). Control of tracheal tubulogenesis by wingless signaling. *Development* **127**, 4433-4442.

Copeland, N. G. and Jenkins, N. A. (1991). Development and applications of a molecular genetic linkage map of the mouse genome. *Trends Genet.* **7**, 113-118.

de Celis, J. F. and Barrio, R. (2000). Function of the *spalt/spalt-related* gene complex in positioning the veins in the *Drosophila* wing. *Mech. Dev.* **91**, 31-41.

de Celis, J. F., Barrio, R. and Kafatos, F. C. (1996). A gene complex acting downstream of *dpp* in *Drosophila* wing morphogenesis. *Nature* **381**, 421-424.

Dudley, A. T., Lyons, K. M. and Robertson, E. J. (1995). A requirement for bone morphogenetic protein-7 during development of the mammalian kidney and eye. *Genes Dev.* **9**, 2795-2807.

Durbec, P., Marcos-Gutierrez, C. V., Kilkenny, C., Grigoriou, M., Wartiowaara, K., Suvanto, P., Smith, D., Ponder, B., Costantini, F., Saarma, M., Sariola, H. and Pachnis, V. (1996). GDNF signalling through the Ret receptor tyrosine kinase. *Nature* **381**, 789-793.

Hata, A., Seoane, J., Lagna, G., Montalvo, E., Hemmati-Brivanlou, A. and Massague, J. (2000). OAZ uses distinct DNA- and protein-binding zinc fingers in separate BMP-Smad and Olf signaling pathways. *Cell* **100**, 229-240.

Jenkins, N. A., Copeland, N. G., Taylor, B. A. and Lee, B. K. (1982). Organization, distribution, and stability of endogenous ecotropic murine leukemia virus DNA sequences in chromosomes of Mus musculus. *J. Virol.* **43**, 26-36.

Jurgens, G. (1988). Head and tail development of the Drosophila embryos involves *spalt*, a novel homeotic gene. *EMBO J.* **7**, 189-196.

Kavety, B., Jenkins, N. A., Fletcher, C. F., Copeland, N. G. and Morgan, J. I. (1994). Genomic structure and mapping of precerebellin and a precerebellin-related gene. *Mol. Brain Res.* **27**, 152-156.

Kispert, A., Vainio, S. and McMahon, A. P. (1998). Wnt-4 is a mesenchymal signal for epithelial transformation of metanephric mesenchyme in the developing kidney. *Development* **125**, 4225-4234.

Kohlhase, J., Schuh, R., Dowe, G., Kuhnlein, R. P., Jackle, H., Schroeder, B., Schulz-Schaeffer, W., Kretzschmar, H. A., Kohler, A., Muller, U., Raab-Vetter, M., Burkhardt, E., Engel, W. and Stick, R. (1996). Isolation, characterization, and organ-specific expression of two novel human zinc finger genes related to the *Drosophila* gene *spalt*. *Genomics* **38**, 291-298.

Kohlhase, J., Wischermann, A., Reichenbach, H., Froster, U. and Engel, W. (1998). Mutations in the *SALL1* putative transcription factor gene cause Townes-Brocks syndrome. *Nat. Genet.* **18**, 81-83.

Kohlhase, J., Hausmann, S., Stojmenovic, G., Dixkens, C., Bink, K., Schulz-Schaeffer, W., Altmann, M. and Engel, W. (1999a). *SALL3*, a new member of the human *spalt*-like gene family, maps to 18q23. *Genomics* **62**, 216-222.

Kohlhase, J., Taschner, P. E., Burfeind, P., Pasche, B., Newman, B., Blanck, C., Breuning, M. H., ten Kate, L. P., Maaswinkel-Mooy, P., Mitulla, B. et al. (1999b). Molecular analysis of *SALL1* mutations in Townes-Brocks syndrome. *Am. J. Hum. Genet.* **64**, 435-445.

Kohlhase, J., Altmann, M., Archangelo, L., Dixkens, C. and Engel, W. (2000). Genomic cloning, chromosomal mapping, and expression analysis of *msal-2*. *Mamm. Genome* **11**, 64-68.

Koseki, C., Herzlinger, D. and al-Awqati, Q. (1991). Integration of embryonic nephrogenic cells carrying a reporter gene into functioning nephrons. *Am. J. Physiol.* **261**, C550-C554.

Kreidberg, J. A., Sariola, H., Loring, J. M., Maeda, M., Pelletier, J., Housman, D. and Jaenisch, R. (1993). WT-1 is required for early kidney development. *Cell* **74**, 679-691.

Kuhnlein, R. P., Frommer, G., Friedrich, M., Gonzalez-Gaitan, M., Weber, A., Wagner-Bernholz, J. F., Gehring, W. J., Jackle, H. and Schuh, R. (1994). *spalt* encodes an evolutionarily conserved zinc finger protein of novel structure which provides homeotic gene function in the head and tail region of the *Drosophila* embryo. *EMBO J.* **13**, 168-179.

Llimargas, M. (2000) wingless and its signalling pathway have common and separable functions during tracheal development. *Development* **127**, 4407-4417.

Lunde, K., Biehs, B., Nauber, U. and Bier, E. (1998) The knirps and knirps-related genes organize development of the second wing vein in *Drosophila*. *Development* **125**, 4145-4154.

Luo, G., Hofmann, C., Bronckers, A. L., Sohocki, M., Bradley, A. and Karsenty, G. (1995). BMP-7 is an inducer of nephrogenesis, and is also required for eye development and skeletal patterning. *Genes Dev.* **9**, 2808-2820.

Marlin, S., Blanchard, S., Slim, R., Lacombe, D., Denoyelle, F., Alessandri, J. L., Calzolari, E., Drouin-Garraud, V., Ferraz, F. G., Fourmaintraux, A. et al. (1999). Townes-Brocks syndrome: detection of a *SALL1* mutation hot spot and evidence for a position effect in one patient. *Hum. Mutat.* **14**, 377-386.

Moore, M. W., Klein, R. D., Farinas, I., Sauer, H., Armanini, M., Phillips,

H., Reichardt, L. F., Ryan, A. M., Carver-Moore, K. and Rosenthal, A. (1996). Renal and neuronal abnormalities in mice lacking GDNF. *Nature* **382**, 76-79.

Moriya, N., Uchiyama, H. and Asashima, M. (1993). Induction of pronephric tubules by activin and retinoic acid in presumptive ectoderm of *Xenopus laevis*. *Dev. Growth Differ.* **35**, 123-128.

Nellen, D., Burke, R., Struhl, G. and Basler, K. (1996). Direct and long-range action of a DPP morphogen gradient. *Cell* **85**, 357-368.

O'Callaghan, M. and Young, I. D. (1995). *Townes-Brocks Syndrome* (ed. D. Donnai and R. Winter). London: Chapman and Hall.

Onuma, Y., Nishinakamura, R., Takahashi, S., Yokota, T. and Asashima, M. (1999). Molecular cloning of a novel Xenopus *spalt* gene (*Xsal-3). Biochem. Biophys. Res. Commun.* **264**, 151-156.

Ott, T., Kaestner, K. H., Monaghan, A. P. and Schutz, G. (1996). The mouse homolog of the region specific homeotic gene *spalt* of *Drosophila* is expressed in the developing nervous system and in mesoderm-derived structures. *Mech. Dev.* **56**, 117-128.

Ott, T., Parrish, M., Bond, K., Schwaeger-Nickolenko, A. and Monaghan, A. P. (2001). A new member of the spalt like zinc finger protein family, Msal3, is expressed in the CNS and sites of epithelial/mesenchymal interaction. *Mech. Dev.* **101**, 203-207.

Pichel, J. G., Shen, L., Sheng, H. Z., Granholm, A. C., Drago, J., Grinberg, A., Lee, E. J., Huang, S. P., Saarma, M., Hoffer, B. J., Sariola, H. and Westphal, H. (1996). Defects in enteric innervation and kidney development in mice lacking GDNF. *Nature* **382**, 73-76.

Rossi, D. L., Hardiman, G., Copeland, N. G., Gilbert, D. J., Jenkins, N., Zlotnik, A. and Bazan, J. F. (1998). Cloning and characterization of a new type of mouse chemokine. *Genomics* **47**, 163-170.

Sanchez, M. P., Silos-Santiago, I., Frisen, J., He, B., Lira, S. A. and Barbacid, M. (1996). Renal agenesis and the absence of enteric neurons in mice lacking GDNF. *Nature* **382**, 70-73.

Sato, A., Asashima, M., Yokota, T. and Nishinakamura, R. (2000). Cloning and expression pattern of a *Xenopus* pronephros-specific gene, *XSMP-30*. *Mech. Dev.* **92**, 273-275.

Saxen, L. (1987). *Organogenesis of the Kidney.* Cambridge: Cambridge University Press.

Schuchardt, A., D'Agati, V., Larsson-Blomberg, L., Costantini, F. and Pachnis, V. (1994). Defects in the kidney and enteric nervous system of mice lacking the tyrosine kinase receptor Ret. *Nature* **367**, 380-383.

Schuchardt, A, D'Agati, V., Pachnis, V. and Costantini, F. (1996). Renal agenesis and hypodysplasia in ret-k- mutant mice result from defects in ureteric bud development. *Development* **122**, 1919-1929.

Stark, K., Vainio, S., Vassileva, G. and McMahon, A. P. (1994). Epithelial transformation of metanephric mesenchyme in the developing kidney regulated by Wnt-4. *Nature* **372**, 679-683.

Torres, M., Gomez-Pardo, E., Dressler, G. R. and Gruss, P. (1995). Pax-2 controls multiple steps of urogenital development. *Development* **121**, 4057-4065.

Trupp, M., Arenas, E., Fainzilber, M., Nilsson, A. S., Sieber, B. A., Grigoriou, M., Kilkenny, C., Salazar-Grueso, E., Pachnis, V. and Arumae, U. (1996). Functional receptor for GDNF encoded by the c-ret proto-oncogene. *Nature* **381**, 785-789.

Uochi, T. and Asashima, M. (1996). Sequential gene expression during pronephric tubule formation in vitro in Xenopus ectoderm. *Dev. Growth Differ.* **38**, 625-635.

Xu, P. X., Adams, J., Peters, H., Brown, M. C., Heaney, S. and Maas, R. (1999). Eya1-deficient mice lack ears and kidneys and show abnormal apoptosis of organ primordia. *Nat. Genet.* **23**, 113-117.